UNIVERSITY OF MARYLAND | NIST
INSTITUTE FOR BIOSCIENCE
& BIOTECHNOLOGY RESEARCH

insight | innovation | application

# EFFECT OF N-TERMINAL METALATION AND LIPID COMPOSITION ON THE ACTIVITY OF ANTIMICROBIAL PISCIDINS IN MEMBRANES

Roderico Acevedo[1], Frank Heinrich[2], Fatih Comert[1] , Vitalii Silin[1], Ananda Chowdhuri[1], Alexander Greenwood[3], Myriam Cotten[3] and Ella Mihailescu[1]

[1]Institute for Bioscience and Biotechnology Research, Rockville, Maryland
[2]NIST Center for Neutron Research, Gaithersburg, Maryland
[3]College of William and Mary, Williamsburg, Virginia

## Introduction

Metal-binding host-defense peptides derived from the innate immune systems of various organisms are promising templates for designing new and potent antibiotics. In this study. piscidins 1 and 3 (P1 & P3) isolated from Hybrid striped bass (*Morone chrysops x Morone saxatilis* are Histidine-rich, amphipathic, cationic, α-helical with a broad-spectrum antimicrobial activity (1). It was recently established that Cu+2 and Ni+2, coordinated through a amino-terminal Copper-Nickel (ATCUN) motif in piscidins 1 and 3, enhances their antimicrobial activity. We seek to understand how microscopic observations macroscopic measurements on their activities are connected with structural observation on the molecular scale, starting at the lipid membrane barrier. Here we combine cell-based assays with a suite of high resolution structural techniques to examine the interactions of the peptides with the lipid membrane at the molecular and the role of metal ions in altering these interactions with the result of enhanced efficacy.

## Peptide structures in lipid bilayers

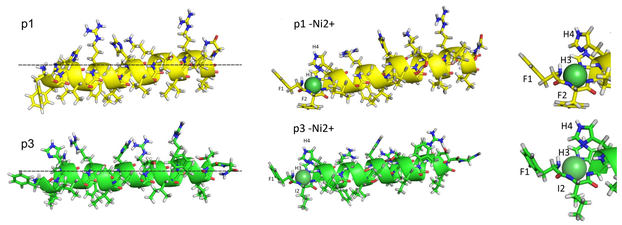


P1: FFHHIFRGIVHVGKTIHRLVTG
P3: FIHHIFRGIVHAGRSIGRFLTG

**Figure 1.** Solid state NMR structures of Piscidins 1 and 3 with and without Nickel-II. They structures were resolved in aligned lipid multilayers of DMPC/DMPG (3:1, molar). The metals (Cu2+ or Ni2+) bind in the histidine-rich N-terminal region (ATCUN motif). The Ni2+ ion (green sphere) is coordinated to the backbone nitrogens of F1, I2, and H3 as well as the imidazole sidechain of H3 in a square-planar geometry (2). Unlike previously reported ATCUN-metal structures, the side chain of the conserved HIS-4 in piscidins appears to also participate in the metal binding. In the halo-state, metal coordination through the ATCUN motif results in the net loss of one positive charge and a partial loss of helical content.

## Piscidin activity on cancer cells

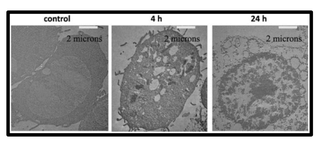


**Figure 2.** Piscidin P1 induces necrosis of HT1080 cancer cells. Control (untreated) cells show a smooth surface, while cells treated with P1 reveal severely damaged cellular membrane. *(Reproduced with permission from Heng-Ju Lin et al., Zool. Sci. 29, 2012)*

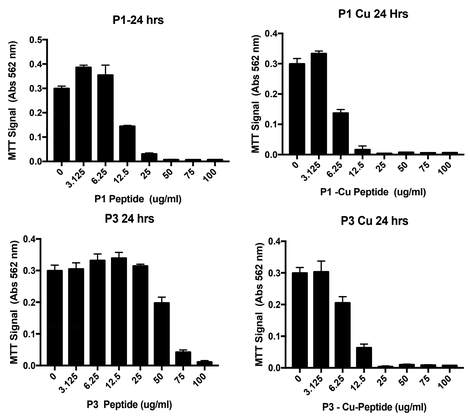


**Figure 3.** Cytotoxicity of P1 and P3 on a lung cancer cell line (A549). Both peptides show excellent cell killing property in the concentration tested, however P1 is more potent than P3. Interestingly, Cu2+ binding restores the efficacy of P3, to a concentration range comparable to P1.

## Lamellar diffraction from oriented lipid bilayers.

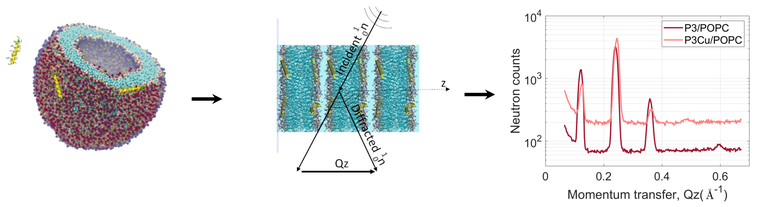


**Figure 4.** From liposomes to oriented bilayers. Peptides are allowed to incubate with preformed liposomes in aqueous buffers and then fused to glass cover slips to form flat bilayer stacks, amenable for diffraction measurements. The samples are hydrated at 93-95% relative humidity from the vapor phase.

## The effect of Cu-II on bilayer and water profiles. Neutron diffraction.

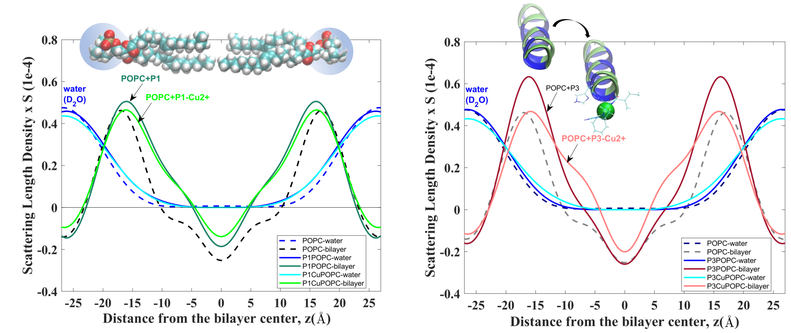


**Figure 5.** The bilayer scattering length density profiles (SLD) in projection to the bilayer normal (z-axis). The orientated samples were prepared in POPC at 1:25 peptide/lipid molar ratio. The more potent P1 is more deeply buried in the hydrocarbon core of the bilayer, compared to the less potent homolog, P3. However, Cu2+ binding in the ATCUN motif increases P3's ability to insert. The depth of insertion correlates directly with the cytotoxicity of P1/P3 on cancer cells, and in particular, the observed gain in potency of P3 upon metal binding (Fig 3). Peptide insertion associates with bilayer distortions and water penetration in the bilayer interior, compromising the integrity and functionality of the membrane barrier.

## The effect of Piscidins on lipid/cholesterol mixtures. X-ray diffraction.

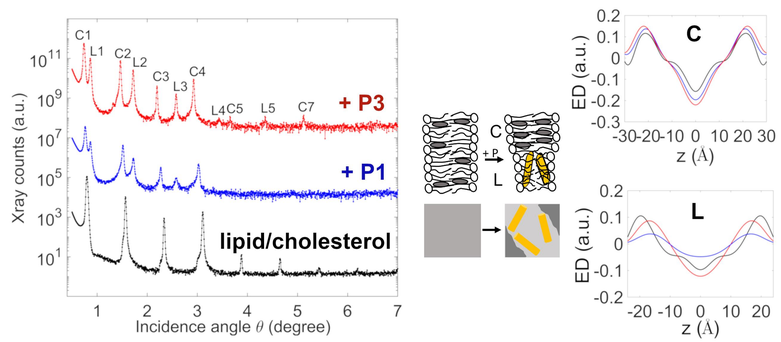


**Figure 6.** In a binary POPC/cholesterol mixture (3:1 molar ratio) Piscidins cause a phase separation into two lipid phases: a cholesterol-rich, liquid ordered phase (C), and a lipid liquid disordered phase (L). While both P1 and P3 partition into the L-phase, P1 produces more severe perturbations to the POPC (L) bilayer structure, as inferred from the electron density profiles (ED, right panel). The bilayer thicknesses including the water layer are 51.05 Å (0.06) for L-P1, 51.52 Å (0.10) for L-P3 and 53.87 Å (0.02) for neat POPC.

## Surface Plasmon Resonance (SPR) and Electrical Impedance Spctroscopy (EIS)

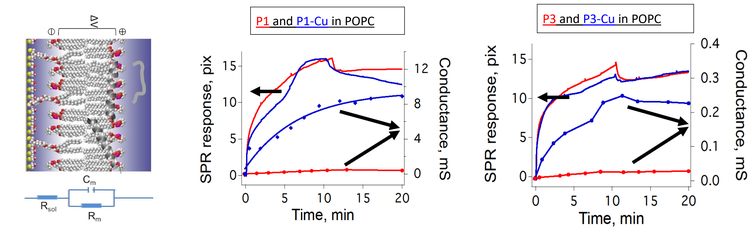


**Figure 7.** Simultaneous SPR/EIS measurements were performed on tBLMs treated with 3 µM P1/P3. While both peptides exhibit similar binding kinetics (by SPR) in both apo- and halo- forms, the bilayer conductance (by EIS) is much higher for P1 than P3, indicating that P1 is more aggressive in forming defects or peptide channels through an otherwise insulating bilayer. The conductance is exacerbated for both P1 and P3 when Cu2+ is bound. Because the kinetics of binding stays roughly unchanged, the differing activities of P1/P3 must rely on their unique interactions with the bilayer's the hydrocarbon region.

## Neutron Reflectometry of tBLMs with Piscidins

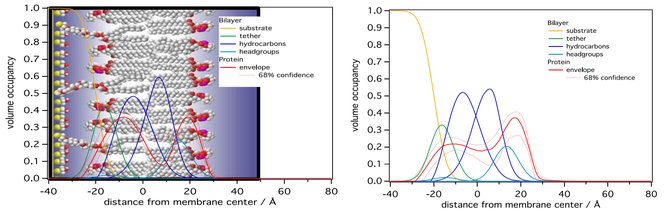


| Parameter | Median ± 68% confidence |
|---|---|
| Tether thickness | 8.7 ± 0.1 Å |
| Hydrocarbon thickness inner lipid leaflet | 13.9 ± 0.7 Å (-0.4 ± 0.2 with protein) |
| Hydrocarbon thickness outer lipid leaflet | 10.6 ± 0.7 Å (-0.4 ± 0.2 with protein) |
| Area per lipid, outer leaflet | 91 ± 7 Å² (with protein) |
| Bilayer completeness | 100 ± 1 % (99 ± 1 % with protein) |
| Amount of membrane-associated protein | 12 ± 2 Å³/Å² |
| Fraction of protein in hydrocarbons | 0.46 ± 0.03 |
| Fraction of protein in headgroups | 0.35 ± 0.02 |
| Fraction of protein in bulk solvent | 0.19 ± 0.02 |

| Parameter | Median ± 68% confidence |
|---|---|
| Tether thickness | 7.5 ± 0.1 Å |
| Hydrocarbon thickness inner lipid leaflet | 12.5 ± 0.8 Å (-0.8 ± 0.3 with protein) |
| Hydrocarbon thickness outer lipid leaflet | 11.1 ± 0.9 Å (-0.8 ± 0.3 with protein) |
| Area per lipid, outer leaflet | 90 ± 8 Å² (with protein) |
| Bilayer completeness | 100 ± 1 % (99 ± 1 % with protein) |
| Amount of membrane-associated protein | 11 ± 2 Å³/Å² |
| Fraction of protein in hydrocarbons | 0.37 ± 0.05 |
| Fraction of protein in headgroups | 0.37 ± 0.02 |
| Fraction of protein in bulk solvent | 0.28 ± 0.03 |

**Figure 8.** The peptides were injected upon a pre-formed tBLM, at a concentration of 3 uM in 20mM Tris buffer , pH7.5. The profiles reveal a higher density of P1-Cu across the hydrocarbon and a more even peptide distribution between the two bilayer leaflets compared to P3-Cu. The somewhat lower incorporation of P3 and the higher density of accumulation on the outer leaflet may be indicative of a lower ability to cross the hydrocarbon barrier, in agreement with observations from cell-based assays (Fig 3), neutron diffraction (Fig 5) and EIS measurements (Fig 7).

## Summary

The two 22-residue, helical, cationic peptides differ only slightly in amino-acid sequences, but P1 is more potent than P3. Solid state NMR showed that P1 and P3 adopt a very similar helical structure in fluid lipid membranes. However, neutron diffraction and reflectometry, in conjunction with electrical impedance spectroscopy (EIS) measurements reveal differing conformations of the two peptides in membrane, depending on lipid composition and peptide metalation state. While (Cu2+) metal binding triggers an increase in the potency of the peptides on cancer cells, it is more dramatically manifested in P3. These changes in potency can be directly correlated with the changes in the peptide conformations and depth of insertions in the membrane barrier. The contrasting behavior of the two AMP homologues offer a unique opportunity to examine the structure-function relationship of ATCUN HDPs.

**Acknowledgements:**
This research received support from the National Science Foundation, award #1714164. The study utilized neutron diffraction facilities at the US National Institute of Standards and Technology (NIST), Gaithersburg, MD. The identification of any commercial product or trade name does not imply endorsement or recommendation by NIST.
We thank Dr. William Stetler-Stevenson (NIH/NCI) for providing the facilities for performing cell cancer assays.

**References**

(1) Perrin, B. S., *J. Am. Chem. Soc.* 2014, 136
(2) Rai, R. K., et al, ChemPhysChem 2019, 20

NIST Center for Neutron Research